EXPERIMENT NO. 3

FLOW MEASUREMENTS AND VISUALIZATION FOR SUPERSONIC FLOW

Submitted by:

Kush Jani

AEROSPACE AND OCEAN ENGINEERING DEPARTMENT

VIRGINIA POLYTECHNIC INSTITUTE AND STATE UNIVERSITY

BLACKSBURG, VIRGINIA

21 NOVEMBER 2025

EXPERIMENT PERFORMED 27 OCTOBER 2025

LAB TEACHING ASSISTANT: NAGA NITISH CHAMALA

I. Abstract

This report contains an investigation into the flow characteristics of a supersonic converging-diverging nozzle with a design Mach number of 1.5 enabled through Virginia Tech's Advanced Propulsion and Power Lab (APPL). The primary objective of this investigation was the validation or invalidation of isentropic flow theory on different flow regimes as well as the qualitative characterization of shock structures associated with over-expanded, under-expanded, and perfectly expanded (design condition) flow regimes. To meet these objectives, a continuous-flow supersonic jet rig was operated at nozzle pressure ratios (NPR) ranging from 2.52 to 4.39 to collect metrics on stagnation pressures enabling for the classification of the flow quantitatively as over-expanded, under-expanded, or perfectly expanded. The efficacy of the quantitative analysis was corroborated by the qualitative analysis performed on the flow through the use of Background-Orientated Schlieren (BOS) visualization as the results showed the presence of sharp oblique shock diamonds for the over-expanded case, a clean flow for the design condition, and expansion fans for the under-expanded case. The results thus confirmed that isentropic theory is accurately capable of predicting the nozzle performance at the design point, but is only a loose approximation for the off-design conditions where non-isentropic shock waves dominate the characteristics of the flow and induce pressure losses. Uncertainty analysis showed a relative error of less than 0.05% due to instrumentation error in the calculated Mach numbers, validating the experimental procedure further and overall demonstrating the success of the investigation in meeting objectives despite limitations caused by environmental conditions during testing due to the corresponding workaround.

FLOW MEASUREMENTS AND VISUALIZATION FOR SUPERSONIC FLOW

Kush Jani[1]
Virginia Tech, Blacksburg, VA 24060

II. Introduction

The goals of this study are:

1. To use experimental measurements and compressible aerodynamic theory to interpret Pitot probe data from subsonic and supersonic flows in order to quantitatively classify flow regimes as over-expanded, under-expanded, or perfectly expanded (design condition).
2. To determine the limitations of isentropic theory used for measuring flow and nozzle characteristics in flows dominated by shock versus flows without shocks.
3. To implement Background-Orientated Schlieren (BOS) visualization to qualitatively determine shock structures and flow characteristics in different supersonic flow regimes and compare with quantitative classifications.
4. To experimentally visualize the creation of a bow shock, normal shock, and artifacts through BOS visualization.

These goals were accomplished using the Virginia Tech Heated Supersonic Jet Rig to generate a continuous supersonic flow through a converging-diverging nozzle in order to generate the necessary flow regimes and gather the necessary Pitot stagnation pressure data as well as capture the flow against a white noise background pattern. The rig and probe are showcased in Fig. 1 and Fig. 2 respectively. The theoretical basis for this experiment is summarized as follows:

Compressible flow through a nozzle is governed by the conservation of mass, momentum, and energy through the complex Navier-Stokes equations. However, by assuming the flow is adiabatic and isentropic, the flow properties can be determined through just the Mach number and stagnation pressures, with the relationship being given by equation

$$\frac{p_0}{p} = \left(1 + \frac{\gamma-1}{2}M^2\right)^{\frac{\gamma}{\gamma-1}} \tag{1}$$

where p_0 is the stagnation pressure, p is the local static pressure, M is the Mach number, and γ is the ratio of specific heats approximated as 1.4 for air. A similar equation exists as well for the ratio between nozzle area A and the critical throat area A^* required to set the flow to a specific Mach number as given by

$$\frac{A}{A^*} = \frac{1}{M}\left[\left(\frac{2}{\gamma+1}\right)\left(1 + \frac{\gamma-1}{2}M^2\right)\right]^{\frac{\gamma+1}{2(\gamma-1)}} \tag{2}$$

From Eq. 1, it can be gleaned that converging-diverging nozzles have a design condition where exit pressure p_e exactly matches the ambient back pressure p_a. However, when operating off the design condition, the pressure mismatch is resolved physically through the creation of shocks which are physical manifestations of discontinuities. When $p_e < p_a$, the flow regime is in an over-expanded case which results in the creation of oblique shocks at the nozzle exit to compress the flow, as well as shock diamonds downstream. Inversely, when $p_e > p_a$, the flow regime is in an under-expanded case which results in the creation of expansion fans at the nozzle exit to expand the flow, as well as shock diamonds downstream like the over-expanded case.

To measure the properties of supersonic flows, a Pitot probe is inserted into the plume. However, the presence of the probe creates a detached bow shock as the flow deaccelerates in a non-isentropic manner across the shock. The stagnation pressure, p_{02}, downstream of such a shock is thus not equivalent to the freestream stagnation pressure p_{01}. However, the ratio between the two stagnation pressures only depends on Mach number and thus can be calculated as given by the Rayleigh-Pitot tube formula

$$\frac{p_{02}}{p_{01}} = \left[\frac{(\gamma+1)M^2}{2+(\gamma-1)M^2}\right]^{\frac{\gamma}{\gamma-1}}\left[\frac{\gamma+1}{2\gamma M^2-(\gamma-1)}\right]^{\frac{1}{\gamma-1}} \tag{3}$$

[1] Undergraduate student, Aerospace & Ocean Engineering Department.

To visualize qualitatively the changes of the flow, this investigation utilizes BOS visualization which itself depends on the Gladstone-Dale relation given by

$$n - 1 = K\rho \tag{4}$$

where n is refractive index, K is the Gladstone-Dale constant, and ρ is fluid density. Thus, it is seen that the index of refraction depends on density of a gas. Thus, since shock waves and expansion fans create large density gradients, Eq. 4 reveals that the gradients will alter the refractive index that defines how light bends for a material and thus enables flow visualization to be done. Specifically, BOS relies on comparing an image of a random background pattern viewed through the flow against a reference image with no flow, with the displacement of the pattern being correlated against various regions to create a comparison that makes the flow structure apparent.

The remainder of this report is as follows: Section III describes the experimental setup, equipment, and techniques used to perform the experiment, including the specific MATLAB codes used to process the pressure data. Section IV describes the results from the experiment by comparing the quantitative pressure data against isentropic theory as well as the qualitative BOS imagery to classify different cases of flow. Finally, Section V contains a discussion regarding the experiment and the insights garnered from the procedure as well as a discussion of the uncertainties tabulated in Appendix A.

III. Apparatus and Techniques

A. Instrumentation

For this investigation, the Virginia Tech Heated Supersonic Jet Rig was used to generate the necessary continuous flow due to its capability of generating supersonic jets at stagnation temperatures up to 700 K, although the experiment conducted only utilized the unheated flow to focus on the unaltered flow structure. The rig itself was set up with a converging-diverging nozzle with a design Mach number of 1.5 that discharged into the lab freely. This rig contains pressure taps and thermocouples, shown in Fig. 3, located in the plenum to measure stagnation pressures, followed by the aforementioned nozzle and a Pitot probe in order to measure the downstream stagnation pressures as well as act like a blunt body in order to generate a detached bow shock. Finally, perpendicular to the flow and located between the nozzle and Pitot probe (offset from the flow centerline to avoid interacting with the flow), is a FLIR camera, as seen in Fig. 4, which faces into the flow and a digital monitor which displays a high contrast white noise pattern to act as the background needed for the BOS visualization. The random pattern is critical to the BOS process as it enables the software to correctly cross-correlate one part of the flow to other parts of the flow which determines the relationship between those regions in terms of displacement and visualizes the result to glean density gradients (and thus shocks and expansion fans).

B. Software

In order to capture the data collected by the probes and control the rig safely, a custom National Instruments LabVIEW interface called *"Facility Monitoring UG Lab.vi"* was used. This software output the real-time measurements made by the probe, specifically the plenum pressure (in psig), atmospheric pressure (in mbar), and calculated the Nozzle Pressure Ratio (NPR) and isentropic Mach number based on the ratio of plenum to ambient pressure. The data used in Section IV is thus the recorded outputs from the LabVIEW interface as shown in Fig. 5. In order to perform the BOS visualization, a MATLAB based particle image velocimetry tool called PIVLab was used by having the software cross-correlate a reference background image captured without flow against images captured under supersonic flow. This allows for the displacement to be calculated as aforementioned, which further allows for the visualization to take place. Finally, post processing of the data measured and recorded by the probes/LabVIEW was performed via the use of custom MATLAB scripts that were based on the Virginia Tech Compressible Aerodynamics Calculators developed by Dr. William Devenport. These scripts are shown in Fig. 6 and Fig. 7 to plot and analyze the data respectively.

C. Experimental Technique

The experiment was conducted through three phases following the set up of the BOS camera to focus on the background monitor and capture of a reference background image without flow. The jet was then activated with the plenum pressure increased to reach desired Mach numbers on the LabVIEW interface of 1.25, 1.5, and 1.65 for the over-expanded, design, and under-expanded flow regimes respectively. At each steady state condition,

images were captured of the LabVIEW interface and for the BOS visualization for subsequent processing in PIVLab. The process for PIVLab analysis involved analyzing the images one pair at a time, with each pair consisting of the still background and the particular Mach case. The images were analyzed for a selected relevant region with the u component in pixels per frame being isolated and visualized on differences of ± 0.2 pixels per frame. During the data collection performed on October 27th, the environmental conditions were unfavorable and prevented a Mach number near 1.65 being reached. The highest Mach achieved was 1.55, which resulted in quantitative and qualitatively distinguishable characteristics during analysis but was not optimal. Consequently, the dataset was supplemented with data provided by lab teaching assistant Roshan Subramanian for an alternate experimental group from October 29th. The alternate dataset was acquired with the same procedure and instrumentation and has been noted as separate throughout Section IV.

IV. Results and Discussion

A. Quantitative Analysis

The quantitative analysis focuses on validating the theoretical relationship between the Nozzle Pressure Ratio (NPR) and the resulting flow regime. NPR represents the ratio between the plenum stagnation pressure p_0 and the atmospheric pressure p. Through use of the MATLAB script shown in Fig. 7, the isentropic flow relations are solved in order to calculate the theoretical exit Mach number M_{exit} and exit static pressure p_{exit} for each case. By comparing the pressure of the jet at the nozzle exit against the surrounding back pressure, the primary cause of shock formation can be identified and thus enable quantitative flow regime classification. Table 1 presents the findings compiled from both original and alternate datasets.

Table 1. Experimental flow conditions.

Source	*NPR*	*Isentropic M*	p_e/p_a	*Regime*
Session 1	2.5214	1.2297	0.68685	Over-Expanded
Session 2	2.5048	1.2245	0.68216	Over-Expanded
Session 1	3.6877	1.5031	1.0045	Design Condition
Session 2	3.7127	1.5078	1.0114	Design Condition
Session 1	3.9926	1.5576	1.0876	Under-Expanded
Session 2	4.3853	1.621	1.1946	Under-Expanded

The data reveals clearly a progression through the various compressible regimes as expected. Namely, the p_e/p_a ratio for the over-expanded case is indeed less than one which is expected in order to have $p_e < p_a$ as covered in the theoretical basis for the investigation. The pressure mismatch thus causes immediate compression of the flow at the nozzle exit forming an oblique shock at the nozzle tip and subsequent shock diamonds. Similarly, the value of p_e/p_a is very nearly one as expected for the design condition due to the very definition of the design condition. Thus the exit pressure of 95.2 kPa is nearly identical to the ambient pressure of 94.8 kPa. As aforementioned, the original experimental session was unable to approach as closely to Mach 1.65 as ideal, although both sessions still demonstrate the expected p_e/p_a ratio behavior of being greater than one in order to have $p_e > p_a$, which was also described in the theoretical basis for under-expanded flow. This results in the formation of strong expansion fans due to the significant energy of the flow that must be spent. Fig. 8 shows the result of the MATLAB code used to plot experimental points against the theoretical isentropic design curve. Notably, the isentropic Mach number is derived based on the ratio of p_e/p_a isentropic and the calculation assumes the total pressure is conserved such that the exit pressure equals the plenum pressure due to the constraints of probe location. In reality, the shock waves created by the over-expanded and under-expanded cases results in a non-isentropic drop in pressure which results in a slight error for the off-design cases. Regardless, the presence of three distinct regimes of flow is apparent. The use of the alternate dataset also enables further verification to the experimental procedure due to the reproducibility being high, as shown by the NPR for the over-expanded case being only 0.02 apart. The plot in Fig. 8 also shows the non-linear nature of Mach number's relation to pressure changes which played a part in preventing the original session from reaching the greater Mach 1.65 needed due to the higher relative pressure differences needed for each additional marginal gain of velocity.

B. Qualitative Analysis

The qualitative analysis of the flow focused on the use of Background-Orientated Schlieren visualization through the use of cross-correlation performed by PIVLab to compare background imagery under no flow to imagery collected at each of the Mach numbers achieved during the investigation. The resulting images are shown in Fig. 9 and Fig. 10 for the original and alternate sessions respectively in the order of ~1.25, ~1.5, and ~1.65 from left to right with color differences being an aesthetic choice to distinguish the sessions.

From the over-expanded case images, it is apparent that a classic shock diamond pattern appears with well-defined periodic regions of compression and expansion, with the sharpness of the features caused by the oblique shocks formed at the nozzle edge. The repeating pattern is a result of the shock waves reflecting off of the freestream layer of the jet's flow. Similarly, these shock diamonds are present in the under-expanded case but are far less well-defined. This is consistent with the theoretical characteristics of the flow as the under-expanded case has expansion fans rather than oblique shocks form at the nozzle edge which interact with the downstream re-compression shocks to create a less sharp gradient compared to the oblique shocks in the over-expanded case. Finally, and most importantly, the design condition is immediately distinguishable through the lack of periodic shock diamonds leaving a relatively clean flow which confirms that the nozzle is expanding flow efficiently to ambient pressure as designed and eliminating adjustment through the natural processes of shocks or expansion fans at the nozzle exit. The flow is not entirely featureless, however, with artifacts apparent on the regions where the flow overlays the Pitot probe and the nozzle. These features are results of the fundamental process behind BOS visualization where the displacement of the nozzle and Pitot probe due to the force of the flow itself causes the BOS visualization to believe the Pitot probe and nozzle are part of the flow that are being displaced far more strongly than the flow itself. However, this is expected and can be ignored in terms of the analysis or classification of the flow itself. Also present in all three cases including the design condition is the formation of a strong detached bow shock caused by the probe itself as it acts like a blunt body in the supersonic freestream. This shock is so strong, it is visible to the naked eye in the raw imagery as seen in Fig. 11 as a blurry region above the Pitot probe. The presence of this shock confirms the flow is supersonic despite the lack of other wave or shock structures in the design condition.

C. Discussion on Potential for Improvements

While the investigation was tremendously successful in meeting all objectives set forth, the only notable limitation was the infeasibility of achieving a Mach closer to 1.65 for the original session although this limitation was offset by the workaround of using the alternative dataset as an additional point of reference. Further possibilities for the experiment could involve the implementation of video to the data collection step in order to examine the time-history evolution of the flow conditions particularly as the flow approaches or deviates away from the design condition.

V. Conclusion

This investigation was greatly successful in investigating the flow characteristics of supersonic flow and visualizing the results in order to classify various flow regimes from over-expanded to design condition to under-expanded. By integrating the quantitative pressure measurements with the qualitative BOS visualization, the experiment was able to corroborate the fundamental compressible flow theories for nozzle performance and shock wave formation as valid while also being able to directly observe the transition from over-expanded to perfectly expanded flow to under-expanded flow in a manner that enabled clear classification of the flow regimes.

The results show that isentropic flow relations are highly accurate for predicting performance of the nozzle at design condition, while only approximating the off-design cases due to the dominance of shock in the flow. At the design NPR of 3.69, the calculated exit pressure ratio was 1.005, which shows that the design condition was able to nearly match the flow at the nozzle to the ambient pressure. The minor discrepancy could be due to any number of physical limitations on the idealized theory including frictional losses or interaction from the downstream detached bow shock caused by the Pitot probe. This quantitative finding was perfectly verified by the BOS visualization which showed a clear flow without the periodic shock diamonds seen in the other cases. Furthermore, the off-design cases created pressure mismatches that on the order of 20 to 30% for the under and

over-expanded cases respectively that necessitated the formation of shocks to return pressure to ambient. The visualization of the sharp oblique shocks in the over-expanded case and the broader expansion fans in the under-expanded case physically prove the non-isentropic behavior of the flow in those regimes. The aforementioned behavior of the Pitot probe as a blunt body also demonstrated the need for the use of the Rayleigh Pitot tube formula rather than relying on the isentropic relations to interpret probe data as the detached bow shock about the probe creates a significant pressure loss that must be tabulated.

The following conclusions can be garnered from this investigation:

1. The flow regimes of a supersonic nozzle are governed primarily by the exit pressure ratio p_e/p_a and through the use of the NPR, quantitative classifications can be made to distinguish between the over-expanded regime, in which $p_e < p_a$ at NPR 2.52, the perfectly expanded regime, in which $p_e \approx p_a$ at NPR 3.69, and the under-expanded regime, in which $p_e > p_a$ at NPR 4.39.
2. Background-Orientated Schlieren (BOS) is an effective process to classify and distinguish between the cases described prior due to the distinguishability of flows with well-defined shock diamonds, relatively clear flow, and loosely defined shock diamonds with expansion fans.
3. Isentropic theory is a valid basis for nozzle design with limitations related to the dominance of shocks in the flow as the investigation found the design condition matches very well with isentropic theory while the more shock dominated off-design cases only were approximated by the theory.
4. The experimental uncertainty, which was primarily a result of the uncertainty in the Scanivalve pressure transducer of $\pm 0.08\%$ as described in Appendix A, was very low enabling a clear capability to classify the flow regimes as the separation in calculated pressure ratios far exceed the instrument error.

From the results of this investigation, the experimental methodology was proven to be highly effective in the measurement and classification of various supersonic flow regimes.

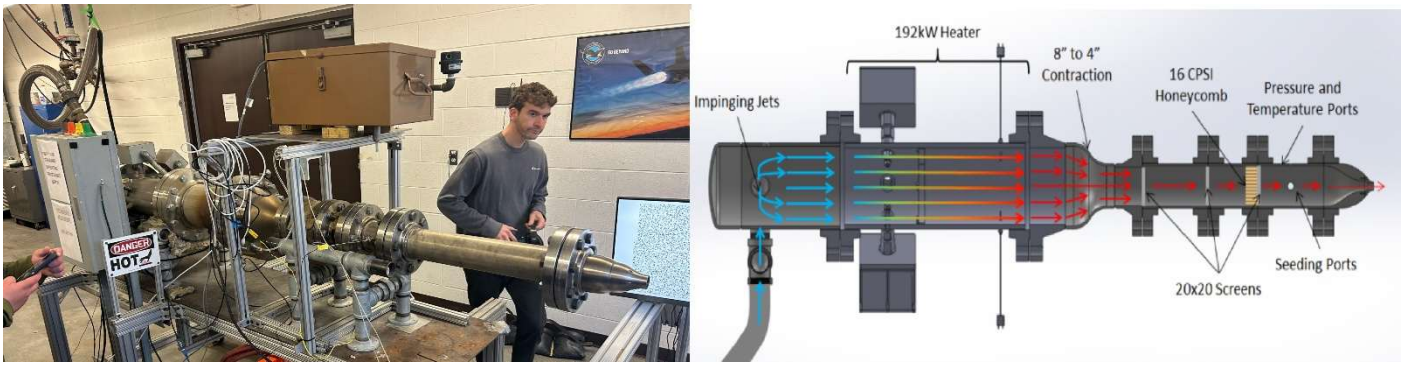

Fig. 1. Virginia Tech Supersonic Heated Jet Rig and Side View Diagram (Weindorf et al. 2024).

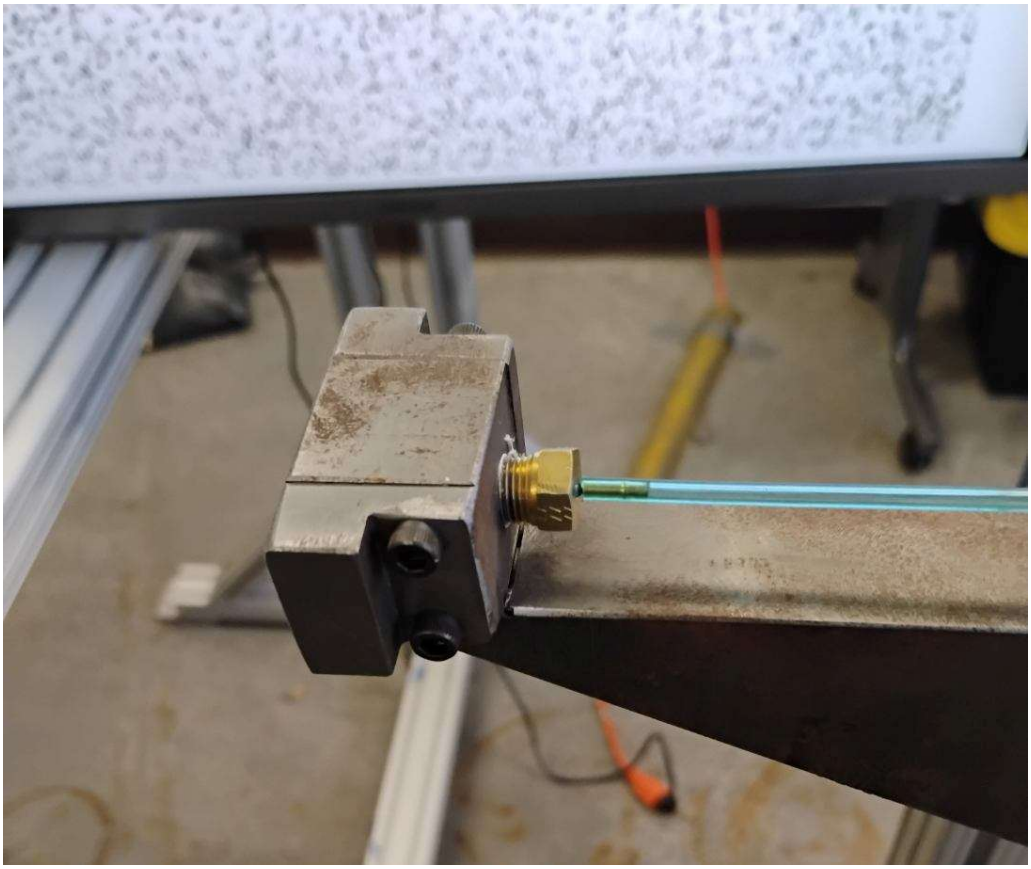

Fig. 2. Pitot Probe.

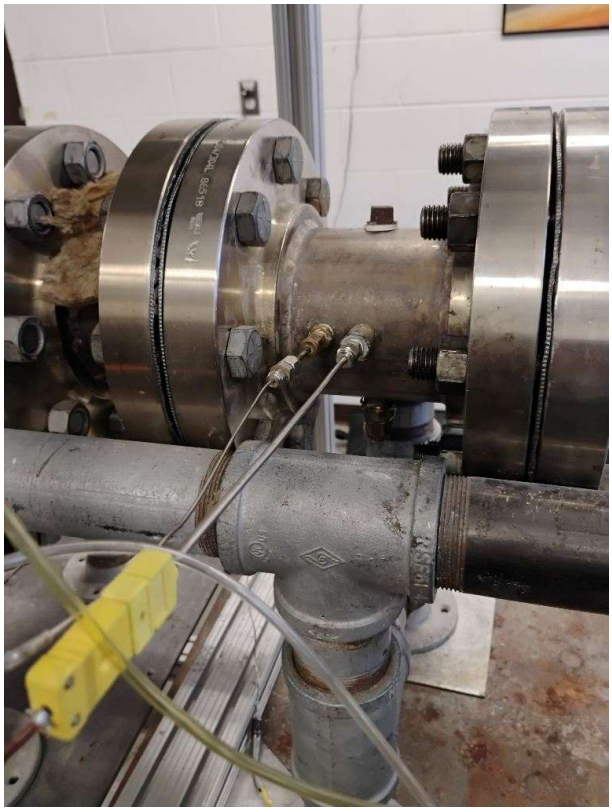

Fig. 3. Pressure Taps and Thermocouple in Plenum.

Fig. 4. FLIR Camera.

Fig. 5. LabVIEW Interface with Bottom Three from Alternate Session (Subramanian 2025)

```
g = 1.4;
NPRtheory = linspace(1.5, 5.2, 100);
mtheory = sqrt((2/(g-1)) * (NPRtheory.^((g-1)/g) - 1));

designM = 1.5;
designNPR = (1 + (g-1)/2 * designM^2)^(g/(g-1));

myNPR = [2.521, 3.688, 3.993];
myM = [1.230, 1.503, 1.558];

altNPR = [2.504, 3.713, 4.385];
altM = [1.225, 1.508, 1.621];

figure
hold on

plot(NPRtheory,mtheory,'--','LineWidth',2,'Color','k')

plot(myNPR, myM, 'o','MarkerSize', 8, 'LineWidth', 1.5,'MarkerFaceColor',
   'k','Color', 'k')
plot(altNPR, altM, 'x', 'MarkerSize',8, 'LineWidth', 1.5,'Color', 'r')

xline(designNPR, ':','LineWidth', 1.8)
yline(designM,':', 'LineWidth',1.8)

xlabel('Nozzle Pressure Ratio (NPR)')
ylabel('Isentropic Mach Number')
title('Experimental Conditions vs Design Theory')
legend('Isentropic Theory', 'My Data', 'Alternate Data', 'Design Point')
grid on
```

Fig. 6. MATLAB Plotting Script.

```
ppsi = [20.9126; 36.9429; 41.134; 20.5646; 37.0862; 46.2811];
mbar = [947.7; 947.7; 947.7; 942.6; 942.6; 942.6];

g = 1.4;
mdes = 1.5;

patm = mbar * 100;
p0 = ppsi * 6894.76 + patm;

npr = p0 ./ patm;
misen = sqrt((2/(g-1)) * (npr.^((g-1)/g) - 1));
merr = abs(misen - mdes) ./ mdes * 100;

prdes = (1 + (g-1)/2 * mdes^2)^(g/(g-1));
pexit = p0 ./ prdes;
pratio = pexit ./ patm;

data = [npr, misen, merr, pexit, pratio];

format short g
disp('   NPR      M_isen    M_err(%)   P_exit(Pa)  P_exit/P_atm')
disp(data)
```

Fig. 7. MATLAB Analysis Script.

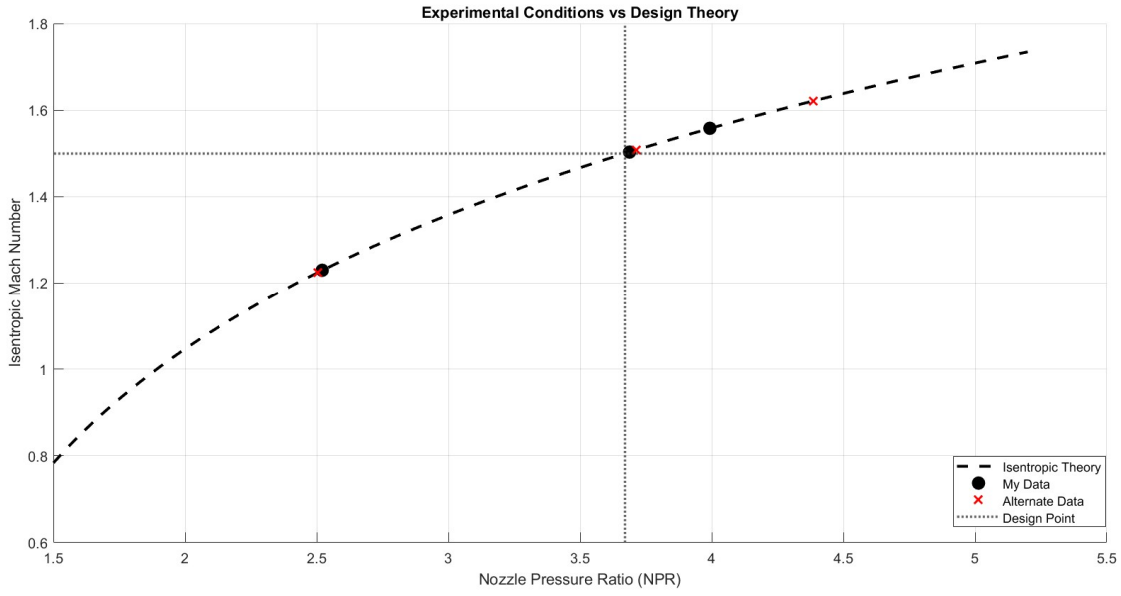

Fig. 8. Plot of Experimental Data Generated via Fig. 6 MATLAB Plotting Code.

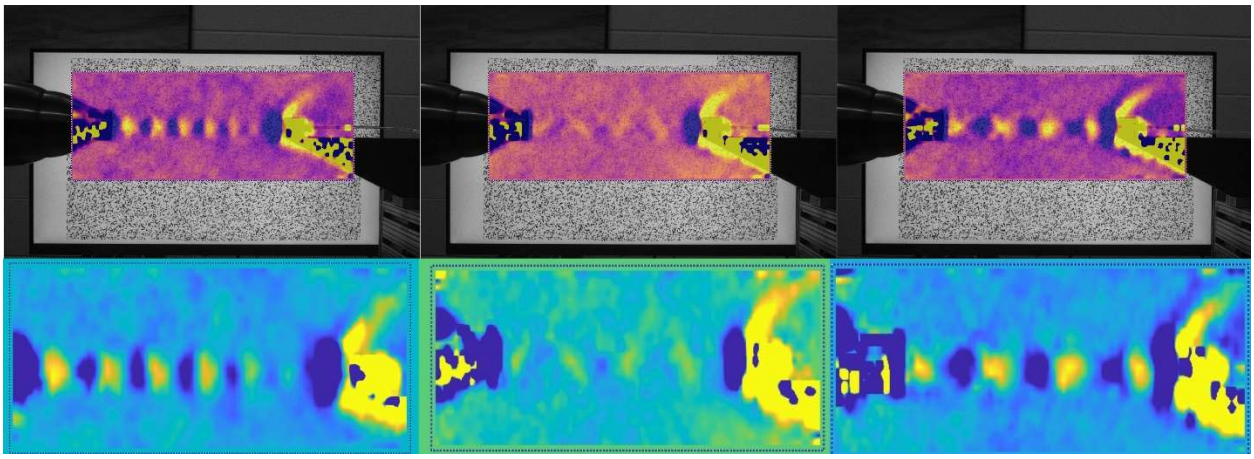

Fig. 9. PIVLab Output from Original Data (M = 1.25, 1.5, 1.65 L to R, Top is Overlay of Bottom on Raw).

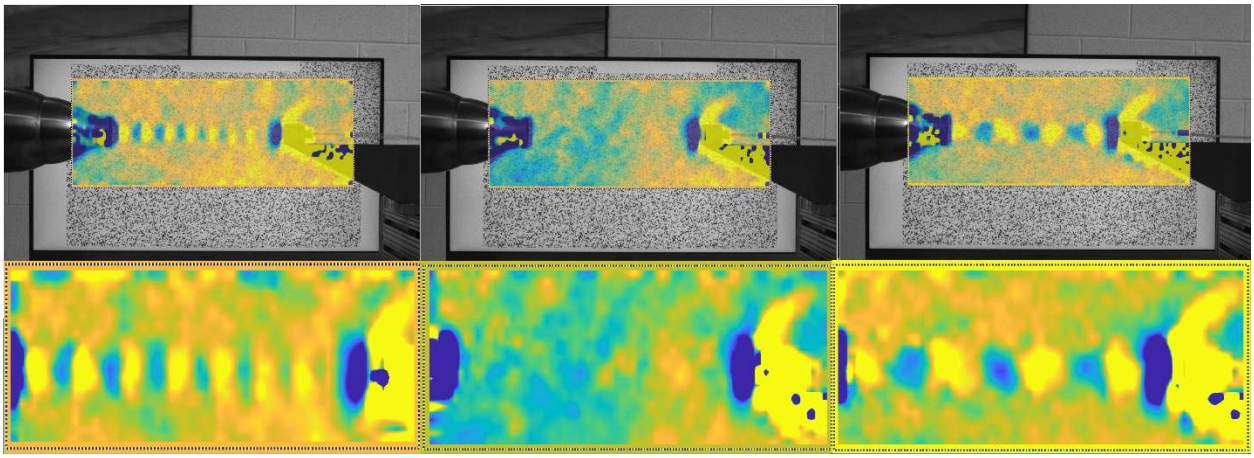

Fig. 10. PIVLab Output from Alternate Data (M = 1.25, 1.5, 1.65 L to R, Top is Overlay of Bottom on Raw).

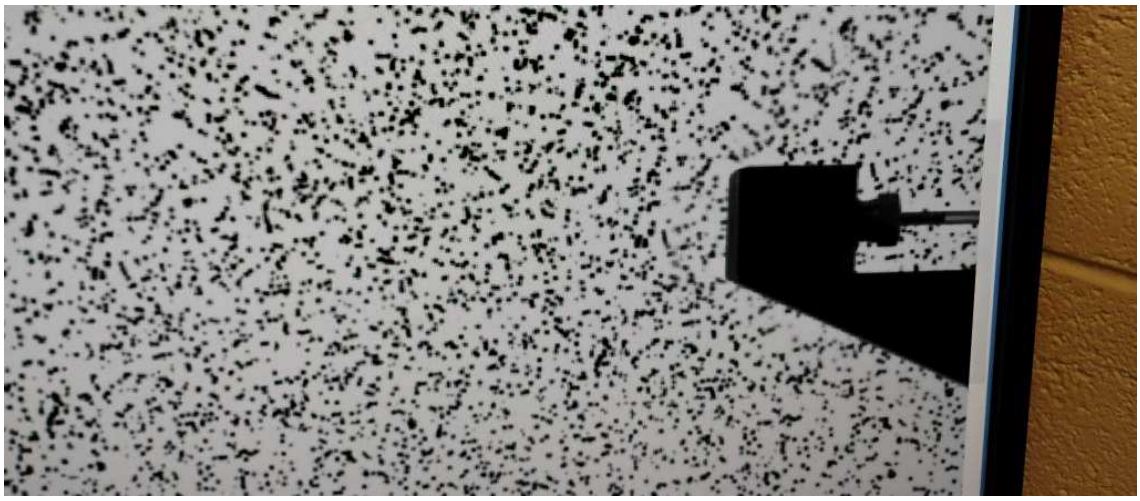

Fig. 11. Detached Bow Shock from Pitot Probe Raw Imagery.

REFERENCES

Weindorf, B., Perez, W., Brooks, D., and Lowe, T., "Flow Measurements and Visualization for Subsonic and Supersonic Flow," AOE 4105 Lab Manual, Rev. 10.10.2024, Virginia Tech, Blacksburg, VA, 2024.

Devenport, W. J., "Compressible Aerodynamics Calculator," Department of Aerospace and Ocean Engineering, Virginia Tech. Available at: https://www.aoe.vt.edu/people/faculty/devenport.html.

Subramanian, R., "Group 1 Pressure Data Snapshots," AOE 4105 Fall 2025 APPL Repository, Virginia Tech, Oct. 2025.

Appendix A

A. Uncertainty Analysis

Uncertainties in derived quantities were calculated using the root-sum-square (RSS) method and reported with 20:1 odds such that a 95% confidence interval is had resulting in a 95% probability that the true value of any such measurement lies within the range defined by the value $\pm$ its uncertainty.

To obtain the uncertainty in for variables dependent on several measured variables, the uncertainties are propagated using the equation

$$\delta(R) = \sqrt{\left(\frac{\partial R}{\partial a}\delta(a)\right)^2 + \left(\frac{\partial R}{\partial b}\delta(b)\right)^2 + \left(\frac{\partial R}{\partial c}\delta(c)\right)^2 + \cdots} \tag{5}$$

where the variables a,b,c… are the variables that R depends on and were measured. The most notable source of uncertainty in this experiment is the pressure measurement from the Scanivalve ZOC17IP/8Px-APC transducer due to the $\pm 0.08\%$ error provided by the manufacturer. Given a range of 0 to 50 psid from the manufacturer as well, a fixed uncertainty ± 0.04 psi or approximately 276 Pa. Another source of uncertainty is the atmospheric pressure reading which was stated to have an estimated uncertainty of ± 0.5 mbar or approximately 50 Pa.

These uncertainties can be propagated via Eq. 5 for the calculation of the NPR and isentropic Mach number performed. The uncertainty in NPR is thus found to be

$$\delta_{NPR} = \sqrt{\left(\frac{1}{p_a}\delta p_0\right)^2 + \left(-\frac{p_0}{p_a^2}\delta p_a\right)^2} \tag{6}$$

and the uncertainty in the isentropic Mach number is found to be

$$\delta M = \left|\frac{dM}{dNPR}\right| \delta NPR \tag{7}$$

Table 2 shows the propagated uncertainties for the design condition which are extremely low, verifying that the instrumentation error is negligible compared to the differences between flow regimes.

Table 2. Uncertainty Propagation for Design Condition of NPR = 3.69.

Variable	*Value*	*Uncertainty*	*Relative Uncertainty*
p_0 (Plenum)	349482	$\pm$276 Pa	0.08%
p_a (Atmosphere)	94770	$\pm$50 Pa	0.05%
NPR	3.6877	$\pm$0.0035	0.09%
Mach Number	1.5031	$\pm$0.0007	0.04%